Parameter Sensitivity Study of Boiling and Two-Phase Flow Models in CFD

Timothy J. Drzewiecki, Isaac M. Asher, Timothy P. Grunloh, Victor E. Petrov, Krzysztof J. Fidkowski, Annalisa Manera and Thomas J. Downar

Reprinted from

The Journal of
Computational Multiphase Flows

Volume 4 · Number 4 · 2012

Multi-Science Publishing

Parameter Sensitivity Study of Boiling and Two-Phase Flow Models in CFD

Timothy J. Drzewiecki[1]*, Isaac M. Asher[2], Timothy P. Grunloh[1], Victor E. Petrov[1], Krzysztof J. Fidkowski[2], Annalisa Manera[1] and Thomas J. Downar[1]
[1]Department of Nuclear Engineering and Radiological Sciences, University of Michigan, 2355 Bonisteel Blvd. Ann Arbor, MI 48109-2105
[2]Department of Aerospace Engineering, University of Michigan

Received: 15 March 2012, Accepted: 6 August 2012

Abstract
This work presents a sensitivity study of boiling and two phase flow models for thermal hydraulics simulations in nuclear reactors. This study quantifies sources of uncertainty and error in these simulations by computing global sensitivities of figures of merit, or output, to model parameters, inputs, and mesh resolution. Results are obtained for the DEBORA benchmark problem of boiling in a channel driven by a heated wall section. Scalar outputs of interest consist of axial pressure drop, average wall temperature in the heated section, average void fraction at the end of the heated section, and the centroid of the radial distribution of the void fraction at the end of the heated test section. Sensitivities to both individual heat fluxes and to the parameters in the models for these heat fluxes are computed.

1. INTRODUCTION

Models for boiling and two-phase flows, particularly in the subcooled regime, are important for thermal hydraulics simulations that support safety and performance analyses of nuclear reactors. Numerous models are currently available for such simulations, e.g. [1,2], many with first-principles justifications [3], but each with a certain number of parameters that can be regarded as tunable or empirically-based. In some cases, these models do not give the same answers and do not necessarily correlate to experiments if they are not independently adjusted for the particular case of interest. A documented example is the failure of high-pressure models applied to subcooled boiling at low pressures [4].

The objective of this study is to take a first step towards quantifying uncertainties in thermal hydraulics simulations by systematically computing global sensitivities of figures of merit, or outputs, to model parameters and inputs. These sensitivities are used to identify parameters that are important for the prediction of the outputs of interest, allowing for a reduction of the input-space dimensionality in future applications such as uncertainty propagation and reliability analysis. Furthermore, for parameters identified as important, the computed sensitivities can be combined with a priori estimates of parameter uncertainty and variability to identify critical parameters and suggest areas of model improvement.

Previous works have considered the sensitivity of boiling models to input parameters and sub-models. Tu and Yeoh [5] studied subcooled boiling at low pressure using Ansys CFX and found that parameters pertaining to partitioning of the wall heat flux, the mean bubble diameter, and the bubble departure diameter have a strong effect on the void fraction. Koncar and Krepper reported similar findings [6,7] using Ansys CFX to investigate turbulent subcooled boiling of a refrigerant. They found that sufficient mesh resolution, the correct bubble diameter, and the inclusion of the bubble lift force were found to be important for ensuring accurate validation. They also pointed out the importance of the bubble size in the bulk flow for the determination of the local liquid subcooling. In addition, the bubble departure diameter has been found to have a considerable effect on the boundary layer turbulence and flow velocity in the boiling region [8, 9]. This result suggestes the need for more sophisticated models than the currently employed single-phase wall functions.

*Corresponding Author: E-mail address: tjdrzew@umich.edu

Krepper and Rzehak [10] presented a sensitivity study of simulations modeling DEBORA experiments [11]. The DEBORA test suite consists of subcooled boiling of a refrigerant in a straight channel geometry with simple boundary conditions. The authors found that the boiling and multiphase flow models in Ansys CFX need to be tuned to the test suite in order to adequately match experiments. Consistently with previous studies, the two key parameters affecting the void fraction distributions were found to be the bubble diameter at departure, also verified by Lo et al [12], and the nucleation site density. Finally, the monodispersed bubble size models used were found to be not capable of predicting the shift of the gas void fraction peak from the wall to the core with increasing inlet temperature.

This sensitivity study proceeds by choosing representative boiling and two-phase flow models in the Eulerian Multiphase CFD code STAR-CD [13]. The DEBORA test case is the benchmark problem that drives this study. The STAR-CD code has been used for validating subcooled boiling models in previous work [14]. The scalar outputs of interest in the present study are the average wall temperature, an integrated void fraction at one axial location, and the axial pressure drop in the channel. Input parameters pertaining to one aspect of the boiling simulations, the wall-to-flow heat transfer model, are varied in a systematic fashion using design-of-experiment capability in the software package DAKOTA. This package is also used to post-process the results.

2. CFD TWO PHASE MODELS AND CONSTITUTIVE RELATIONS

The STAR-CD Eulerian two-phase solver tracks the mass, momentum, and energy of the liquid and vapor phases in each computational cell. A modified k-ε model is used to model the turbulence in the continuous phase, with an algebraic formula used to model the turbulence in the dispersed phase. Full details of the Eulerian two-phase flow models in STAR-CD can be found in the STAR-CD manual [13]. The mass, momentum, and energy transport equations are given below.

Mass

$$\frac{\partial}{\partial t}\left(\alpha_k \rho_k\right)+\nabla\cdot\left(\alpha_k \rho_k u_k\right)=\sum_{j=1}^{N}\left(\dot{m}_{jk}-\dot{m}_{kj}\right) \tag{1}$$

Momentum

$$\frac{\partial}{\partial t}\left(\alpha_k \rho_k \vec{u}_k\right)+\nabla\cdot\left(\alpha_k \rho_k \vec{u}_k \vec{u}_k\right)=-\alpha_k \nabla p+\alpha_k \rho_k \vec{g}+\nabla\cdot\alpha_k\left(\tau_k+\tau_k^t\right)+M_k \tag{2}$$

$$M=F_D+F_{TD}+F_L+F_{VM}+\sum_{j=1}^{N}\left(\dot{m}_{jk}\vec{u}_j-\dot{m}_{kj}\vec{u}_k\right) \tag{3}$$

Energy

$$\frac{\partial}{\partial t}\left(\alpha_k \rho_k h_k\right)+\nabla\cdot\left(\alpha_k \rho_k \vec{u}_k h_k\right)-\nabla\cdot\left[\alpha_k\left(\lambda_k \nabla T_k+\frac{\mu_t}{\sigma_h}\nabla h_k\right)\right]=Q_k \tag{4}$$

$$Q_k=\alpha_k\frac{Dp_k}{Dt}+\alpha_k\left(\tau_k+\tau_k^t\right):\nabla\vec{u}_k+\sum_{i\neq k}Q_{ki}+\sum_{(ik)}Q_k^{(ik)}+\sum_{i\neq k}\left(m_{ki}h_k^{(ik)}-m_{ik}h_k\right) \tag{5}$$

Additional constitutive equations are implemented in order to close the model. These relationships can be classified into areas of phase-to-phase momentum transfer, phase-to-phase heat and mass transfer, and wall-to-flow heat transfer.

2.1. Phase-to-phase momentum transfer

From Eq. 3, models are needed to determine the drag force, F_D, turbulent dispersion force, F_{TD}, the lift force, F_L, and the virtual mass force, F_{VM}. The drag force is calculated using Eq. 6, where the coefficient, A_D, and relative velocity is, u_r, are given by Eq. 7 and Eq. 8 respectively.

$$F_D = A_D \vec{u}_r \tag{6}$$

$$A_D = \frac{3}{4}\frac{\alpha_d \rho_c C_D}{d}\left|\vec{u}_r\right| \tag{7}$$

$$\vec{u}_r = \vec{u}_c - \vec{u}_d \tag{8}$$

Determination of the bubble drag coefficient is obtained using the correlation of Wang [15], given by Eq. 9 and the coefficients provided by Wang, with a,b,c dependent on Re_d.

$$C_D = \exp\left[a + b\ln \mathrm{Re}_d + c\left(\ln \mathrm{Re}_d\right)^2\right] \tag{9}$$

The turbulent dispersion force is given by Eq. 10 and utilizes terms previously defined for the determination of the drag force [16]. The turbulent Prandtl number is set to 1.0.

$$F_{TD} = -A_D \frac{\upsilon_c^t}{\sigma_\alpha}\left[\frac{\nabla \alpha_c}{\alpha_c} - \frac{\nabla \alpha_d}{\alpha_d}\right] \tag{10}$$

The lift force is given by Eq. 11 with the lift coefficient, C_L, set to -0.03.

$$F_L = C_L \alpha_d \rho_c \left[\vec{u}_r \times \left(\nabla \times \vec{u}_r\right)\right] \tag{11}$$

The virtual mass force is calculated using Eq. 12 with a virtual mass coefficient of 0.5.

$$F_{VM} = C_{VM} \alpha_d \rho_c \left[\frac{D\vec{u}_c}{Dt} - \frac{D\vec{u}_d}{Dt}\right] \tag{12}$$

2.2. Phase-to-phase heat and mass transfer

Heat transfer from the liquid to the bubble interface is determined using Eq. 13, where the heat transfer coefficient is determined using the model of Ranz and Marshall [17], see Eq. 14.

$$\dot{q}_l = h_l A_d \left(T_l - T_{sat}\right) \tag{13}$$

$$Nu_l = 2 + 0.6\,\mathrm{Re}_d^{0.5}\,\mathrm{Pr}_l^{0.3} \tag{14}$$

A similar relationship is used for the heat transfer from the vapor to the bubble interface, see Eq. 15. However, the heat transfer coefficient is obtained by using a constant Nusselt number of 26.

$$\dot{q}_g = h_g A_d \left(T_g - T_{sat}\right) \tag{15}$$

The relationships for phase-to-phase heat transfer are then utilized to determine the water to steam mass transfer rate given by Eq. 16.

$$\dot{m} = \left(\dot{q}_l + \dot{q}_g\right) / h_{fg} \tag{16}$$

In determining the phase-to-phase heat transfer, the interfacial area concentration is required. In place of a more sophisticated treatment for interfacial area, such as the interfacial area transport

model developed by Ishii [18], the interfacial area concentration is obtained by utilizing the void fraction and Sauter mean diameter. This expression is given by Eq. 17.

$$A_d = 6\alpha_g / d \tag{17}$$

In a manner similar to Kurul and Podowksi [1] it is assumed that the bubble diameter is a function of the local liquid subcooling. The expression for the Sauter mean diameter is given by Eq. 18 with d_0=0.15 mm, d_1=2 mm, ΔT_0=13.5 K, and ΔT_1=-5 K.

$$d = \frac{d_1\left(\Delta T_{sub} - \Delta T_0\right) + d_0\left(\Delta T_1 - \Delta T_{sub}\right)}{\left(\Delta T_1 - \Delta T_0\right)} \tag{18}$$

2.3. Wall-to-phase heat transfer

The heat transfer from the wall to the fluid in subcooled boiling consists of three parts: single phase convective heat transfer, evaporative heat transfer, and the quenching heat transfer (see Eq. 19).

$$q_T'' = q_c'' + q_e'' + q_q'' \tag{19}$$

The evaporative heat flux is obtained using Eq. 20, where n'' is the nucleation site density and f is the bubble departure frequency.

$$q_e'' = \frac{\pi d_w^3}{6}\rho_g h_{fg} f n'' \tag{20}$$

The nucleation site density is obtained using Eq. 21 with m=185.0 and p=1.805, and the bubble departure frequency is obtained using Eq. 22.

$$n'' = \left(m\Delta T_{\sup}\right)^p \tag{21}$$

$$f = \sqrt{\frac{4}{3}\frac{g\left(\rho_l - \rho_g\right)}{d_w \rho_l}} \tag{22}$$

The wall is broken up into two regions: A_e is the area fraction where evaporative heat transfer occurs and A_c is the area fraction where single phase convective heat transfer occurs. The area fraction of evaporative heat transfer is determined using Eq. 23, with the coefficient, F_A, set to 2.0.

$$A_e = F_A\left(\frac{\pi}{4}d_w^2\right)n'' \tag{23}$$

With the evaporative area fraction, the single-phase convective heat flux and quenching heat flux are obtained using Eq. 24 and Eq. 25, respectively. The single-phase heat transfer coefficient is obtained using wall functions associated with the k-ε turbulence model. The quenching heat transfer coefficient is obtained using the model of Del Valle and Kenning, Eq. 26, with wait time determined by Eq. 27.

$$q_c'' = h_c\left(1 - A_e\right)\left(T_{wall} - T_l\right) \tag{24}$$

$$q_q'' = h_q A_e\left(T_{wall} - T_l\right) \tag{25}$$

$$h_q = 2f\sqrt{t_w \rho_l C_{p,l} \lambda_l / \pi} \tag{26}$$

$$t_w = 0.8 / f \tag{27}$$

A bubble departure size is needed to determine the evaporative heat flux and evaporative area fraction. The expression of Tolubinsky and Kostanczuk [19], obtained for water at a liquid velocity of 0.2 m/s, is utilized. This expression, given by Eq. 28, utilizes a coefficient, d_0, of 0.6 mm which is modified from the original value of 1.4 mm. A value for ΔT_0 of 45 K is consistent with the original reference.

$$d_w = d_0 \exp\left(-\Delta T_{sub} / \Delta T_0\right) \tag{28}$$

3. TEST CASE AND APPLICATIONS

One of the CASL T/H challenge problems involves using CFD to identify regions where subcooled boiling can occur. Therefore, a test case was chosen to assess the performance of CFD to model subcooled boiling. The DEBORA experiment was performed at the Commissariat à l'Energie Atomique. In this experiment, R-12 is used as the working fluid to simulate pressurized water reactor conditions under low pressure. Liquid R-12 flows upward inside a vertical pipe having an internal diameter equal to 19.2 mm. The whole pipe can be divided axially into three parts: the adiabatic inlet section (1 m length), the heated section (3.5 m length), and the adiabatic outlet section (≈0.5 m length). Vapor bubbles are generated by nucleation onto the wall surface and condense into the subcooled liquid when they are far from the wall. In this experiment, local measurements can be performed with a sensor displaced in the radial direction only [11]. At the end of the heated section, the radial profiles of the void fraction and bubble diameter have been measured by means of an optical probe, and liquid temperature has been measured by thermocouples.

The STAR-CD model of the DEBORA experiment utilizes an axisymmetric mesh, a portion of which is shown in Fig. 1. The system pressure is 1.459 MPa with inlet conditions specified at an inlet velocity of 1.72 m/s and void fraction of 0.001. The wall heat flux is 76.24 kW/m^2. Implementation of the wall-to-fluid heat transfer models is accomplished through the use Fortran subroutines that are implanted into STAR-CD through user-defined "ufiles" [13].

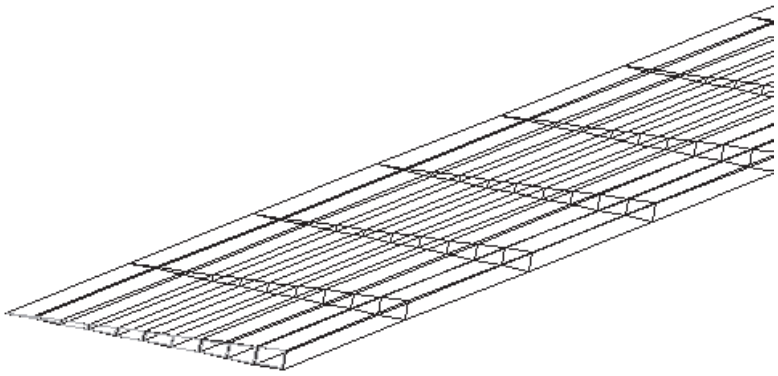

Figure 1. Portion of the mesh used in the STAR-CD model.

4. UNCERTAINTY QUANTIFICATION METHODS AND CODES

A Monte-Carlo approach was used to perform to the sensitivity study. Latin-Hypercube sampling, which attempts to ensure that the parameter space is fully explored, was used to determine the appropriate values of the parameters to simulate.

For both boiling models tested, all of the parameters were varied together in a monolithic sensitivity study. We note that due to the high-level treatment of some of the models, such as heat-partitioning boiling, any magnification of uncertainties in sub-models was ignored. That is, a

variation in heat transfer of ±30% may imply a variation of some empirical constant by 0.001%, or possibly 200%, depending on the structure of the sub-model.

For each parameter, a prior probability distribution was assumed. A fixed percentage variation was used in the absence of comprehensive a priori information about the ranges or distributions of the model parameters. In addition, each parameter was assumed to have a uniform probability density function within that range.

The Sandia DAKOTA sensitivity and uncertainty analysis software was used to generate the Latin-Hypercube samples and execute STAR-CD with the modified parameters. STAR-CD only provides point-wise outputs, and these were stored in text files that were post-processed to yield the integrated outputs of interest. The integration was performed using a third-order method for the evenly-spaced points in the axial direction. In the radial direction, the mesh size varies, so the simpler midpoint method was used.

5. PARAMETER AND MODEL SELECTION

5.1. Inputs

The goal of the study was to find the most important uncertainties in the parameters of approximate or empirical relations used in the STAR-CD two-phase flow model. Parameters were chosen to split up the two-phase flow model into a few major components. During initial prototyping, one parameter in each component was varied, and in subsequent studies the models and sub-models in the important components were varied. Each of these components may comprise a number of models, correlations, and empirical factors, but including all of those parameters in a sensitivity study would be prohibitively expensive. The dimensionality of the problem was reduced so that important components could be isolated for further study. The components involving uncertain parameters were as follows:

- gas-liquid heat and mass transfer
- gas-liquid momentum transfer (drag, lift, virtual mass, and turbulent dispersion forces)
- void fraction, interfacial area
- wall-to-flow heat transfer (heat partitioning model or Chen's correlation)
- turbulence

It was not possible to vary all of the components directly. For example the user cannot place a pre-multiplier on the drag force directly. However, the routine that calculates the coefficient of drag can be altered by the user. Thus, we chose a set of parameters that were available for user-specification such that each component was linearly related to at least one parameter. The parameters actually varied and their ranges are described in Table 1.

Table 1. Summary of parameters for sensitivity study

Parameter	Baseline	Variation	Comments
d	Kurul-Podowski	±30%	
K_1	0.6 (Ranz-Marshall)	±30%	Encompasses experimental data
Nu_g	26	[2,30]	Conduction sets lower bound
C_d	Wang correlation	±30%	
σ_a	0.9	±30%	
C_L	-0.03	±30%	Tomiyama correlation not used
C_{VM}	0.5	[0,1]	Ishii and Mishima
C_μ	1.0	±30%	Scaling factor for liquid turbulent viscosity
C_t	1.0	±30%	Scaling factor for gas/liquid turbulent viscosity ratio
$C_{n''}$	1.0	±30%	Scaling factor for nucleation site density
C_{q_e}	1.0	±30%	Scaling factor for evaporative heat flux
C_{q_q}	1.0	±30%	Scaling factor for quenching heat flux
C_{chen}	0.00122	±30%	Coefficient in Chen's boiling correlation

Figure 3 and Figure 4 show how these parameters (boxed) are used in the various models. We could not avoid the fact that some parameters affected multiple components simultaneously. However, the effects of each component can be deduced from the effects of the parameters and the relationships described in Figure 3 and Figure 4.

5.2. Outputs

Four outputs of engineering relevance are considered for the sensitivity study. The first output is pressure drop over the channel, which should be equal to inlet pressure because of the proscribed outlet pressure $p_{\text{outlet}} = 0$.

$$\Delta p = \bar{p}(z = 5m) - \bar{p}(z = 0m) = -\bar{p}(z = 0m) = -\frac{1}{\mathrm{A}}\int p(r, z = 0m)dA$$

Note that strictly speaking the differential element should be *rdr*, but the variations in pressure in the radial direction are small. The second output is the average wall temperature in the heated section

$$\bar{T}_w = \frac{1}{3.5m}\int_{z=1m}^{z=4.5m} T_w(z)dz$$

The third output is the radial-average void fraction at the end of the heated section

$$\bar{\alpha}_g = \frac{1}{\mathrm{A}}\int \alpha_g(r, z = 4.5m)\, dA$$

Finally, the fourth output is the centroid of the radial void fraction profile

$$\bar{r}_{\alpha_g} = \frac{1}{\mathrm{A}\bar{\alpha}_g}\int \alpha_g(r, z = 4.5m) r dA$$

6. RESULTS

For each parameter, results of the sensitivity study yielded a correlation of that parameter to the four outputs. This correlation is a measure of how strongly the output depends on the parameter. A correlation coefficient of almost one (or minus one) means that the parameter is responsible for most of the variation in the output. It does not give information about how sensitive the physical output is to that parameter.

The correlation coefficients between the parameters should be zero if DAKOTA chose them independently. This is satisfied because all of the correlations were less than in absolute value. In the heat flux partitioning model study there were 12 parameters and 836 total runs, of which 336 did not converge to the pre-set residual tolerance of 10^{-7}, but instead reached the maximum of 2500 iterations. The study with Chen's correlation had 10 parameters and 600 total runs, of which 155 did not reach the residual tolerance. Figure 5 shows the histogram of the residuals for both studies, which indicates that most runs were well converged, even if they did not reach the somewhat strict residual tolerance. Some of the data points did contain large residuals, and these were manually removed before post-processing. Figure 9 and Figure 10 show that there are no major outliers in the outputs.

6.1. Mesh Convergence

A mesh convergence study was performed in an effort to produce a quality base model for use in the sensitivity study. In the process of performing the mesh convergence study, it was found that the size of the first mesh off the wall, and mesh anisotropy had significant impact on the results. In particular, the first mesh adjacent to the pipe is set to a width of 0.15mm which results in a y+ that varies from 30 to 60 along the length of the pipe. In an effort to preserve mesh anisotropy, a mesh

convergence study was performed using mesh sizes of 200x11 (axial mesh by radial mesh), 260x14, 300x16, 340x18, 360x19, 380x20, and 400x21. It is noted that fixing the mesh at the wall prevents mesh anisotropy from being preserved at the first two cells off the wall, but the remaining cells maintain an aspect ratio of 20. The results from the convergence study are provided in Figure 2 and do not demonstrate a clear asymptotic convergence, particularly in the pressure drop. The average wall temperature and the void fraction have approached a region where little variation is observed, but the pressure drop appears to decrease linearly with refinement. Further refinement of the mesh resulted in iterative convergence problems and could not be performed.

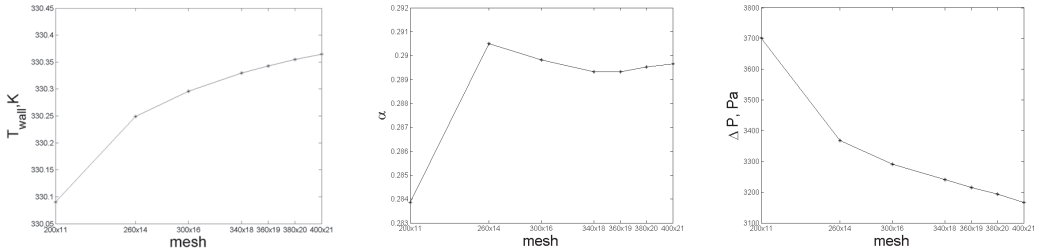

Figure 2. Figures of merit observed in convergence study: (a) $T_{wall,}$ (b) void fraction at end of heated section, and (c) pressure drop.

Given plausible explanations for lack of textbook asymptotic convergence, but finite resources to investigate all possibilities, the authors resolved to proceed with the sensitivity study. The baseline mesh used was a relatively coarse one, 800 axial cells by 11 radial cells, chosen based on robustness and run time considerations given the large number of required runs.

6.2. Heat partitioning model

Figure 6 shows, for each parameter, the correlation coefficients with respect to the four outputs. From this figure we can make a few remarks. First, the most important parameters are bubble departure diameter (d), liquid Nusselt number (K_1), turbulent viscosity coefficients (C_μ and C_t), nucleation site density (n''), and evaporative heat flux (q_e). The liquid turbulent viscosity (C_μ) is mainly important for the pressure drop, and the virtual mass coefficient is moderately important. The wall-to-flow model in Figure 3 shows that n'' affects all of the heat fluxes equally (since it is linearly related to each of them). From the correlation coefficients, it is clear that n'' and have the same effect, whereas has no effect. Thus we conclude that is in this case acting only through q_e, and q_c has little effect.

Also, we note that the correlation coefficients with the void fraction have the opposite sign as those for the pressure drop and the centroid of the void fraction profile. Thus, in general, higher void fractions imply lower Δp and more bubbles near the center of the pipe. Although the STAR-CD model cannot predict the void fraction peak moving away from the wall, it does successfully model the fact that more bubbles tend to be located in the middle of the pipe with higher temperatures and more boiling [10]. We can further see this by looking at the correlations between the outputs. The void fraction $\bar{\alpha}_g$ has a correlation coefficient of –0.77 with respect to Δp and –0.82 with respect to $\bar{r}\,\alpha_g$. Note that this trend is not true of the gas turbulent viscosity parameter C_t. When C_t increases, $\bar{r}\,\alpha_g$ decreases as expected, but Δp increases. This may be due to the increased mixing in the gas phase that occurs with higher C_t, which would lead to more and larger bubbles further from the wall, which leads to a larger pressure drop.

The left plot of Figure 8 shows, for each output, the correlations of all of the parameters. First, the average wall temperature is almost exclusively affected by the evaporative heat flux (as mentioned above, we can infer that n'' acts only through q_e).

Second, the gas Nusselt number Nu_g, the turbulent Prandtl number σ_a, and the lift coefficient C_L have little effect on any of the outputs. It is interesting to note that the liquid Nusselt number has a relatively strong effect, although the gas Nusselt number does not. This implies that there is

little condensation going on, and heat is mostly being transferred from the liquid to the gas. Also, the relative unimportance of σ_a implies that bubble drag due to turbulent eddies is of little importance. The insignificance of C_L can be partially attributed to the fact that the values were quite small, but the other bubble forces (turbulent dispersion, drag, and virtual mass) had relatively small effects on the outputs.

Third, the bubble departure diameter () has a strong effect on all of the outputs except the average wall temperature. This observation has been made previously, most recently by Lo et al [20].

Overall, we can give the following summary

1. Bubble departure diameter is the most important parameter overall.
2. Evaporative heat flux is the only important parameter for average wall temperature, and is important for the other outputs as well.
3. Liquid-to-gas heat transfer and turbulence modeling are important.
4. Momentum transfer is overall not as important.

Figure 9 shows some scatter plots of the data. From these we can identify the physical sensitivities as well. The variations of the outputs are shown in Table 2. From these variations we see that Δp is not predicted well, and that $\bar{\alpha}_g$ is predicted to a coarse engineering accuracy. The average wall temperature is predicted relatively well. Although $\bar{r}_{\alpha_g}$ seems to be predicted well here, we know that the void fraction profile is not accurate [10]. The apparent small sensitivity of $\bar{r}_{\alpha_g}$ implies that varying (or tuning) the parameters will probably not significantly improve the prediction of the void fraction profile. Again, a possible exception to this is the lift coefficient, which was not varied significantly in this study, but which could have a strong effect on the void fraction centroid.

Table 2. Overall variation of outputs

Output	Approximate range
Δp	2000 – 4000 Pa
$\bar{T}_w$	334.5 – 337 K
$\bar{\alpha}_g$	0.13 – 0.18
$\bar{r}_{\alpha_g}$	7 – 8mm

6.3. Chen s correlation

The results for the Chen's correlation study are quite similar to those of the heat partitioning model study. In particular, Figure 7 shows all of the same patterns as Figure 6, with the Chen's correlation parameter having a large impact on the wall temperature $\bar{T}_w$. One exception is that C_{chen} had little impact on the other outputs, compared to the wall boiling parameters in the heat partitioning model.

From Figure 7, we can see that C_{chen} is more strongly correlated to the wall temperature than q_e was, which is consistent with the fact that Chen's correlation is a simpler wall boiling model than heat partitioning. Also, it is again clear that C_{chen} had less of an impact on the other outputs than does q_e. All other correlations are nearly the same between the two studies.

Figure Figure 10 shows a few scatter plots of the data. The strong correlation between C_{chen} and $\bar{T}_w$ can be seen, along with the overall ranges of the outputs, which are similar to those in Table 2.

The heat partitioning model for wall boiling is complicated and therefore affects the overall solution and the outputs Δp, $\bar{\alpha}_g$ and $\bar{r}_{\alpha_g}$. The simpler Chen's correlation has less interaction with the rest of the solution. Therefore, it strongly affects the wall temperature, but does not affect the rest of the simulation. As a final note, we have seen that small values of C_{VM} tend to cause problems with iterative convergence. This can be seen in the upper-middle plot of Figure 10, where the cases that did not reach the residual tolerance tend to be clustered toward lower values of C_{VM}. Also, many of the cases that did not converge at all had very low values of C_{VM}. Figure 5 shows that the momentum equation generally has the largest residual.

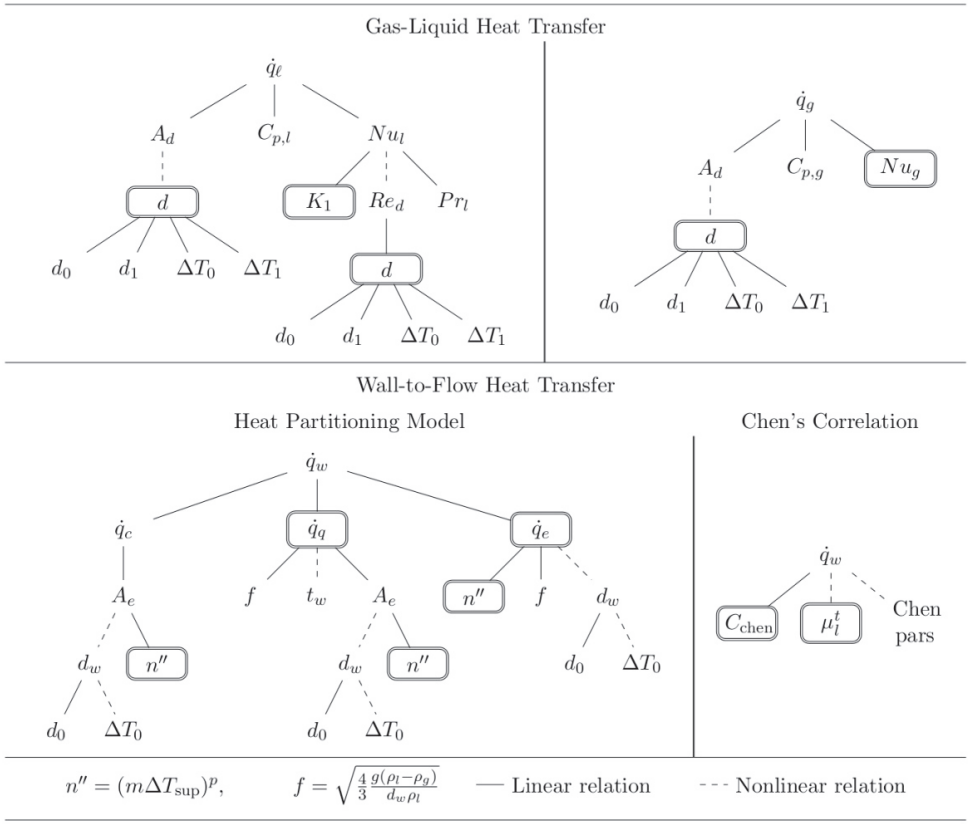

Figure 3. Heat transfer models and parameters in STAR-CD

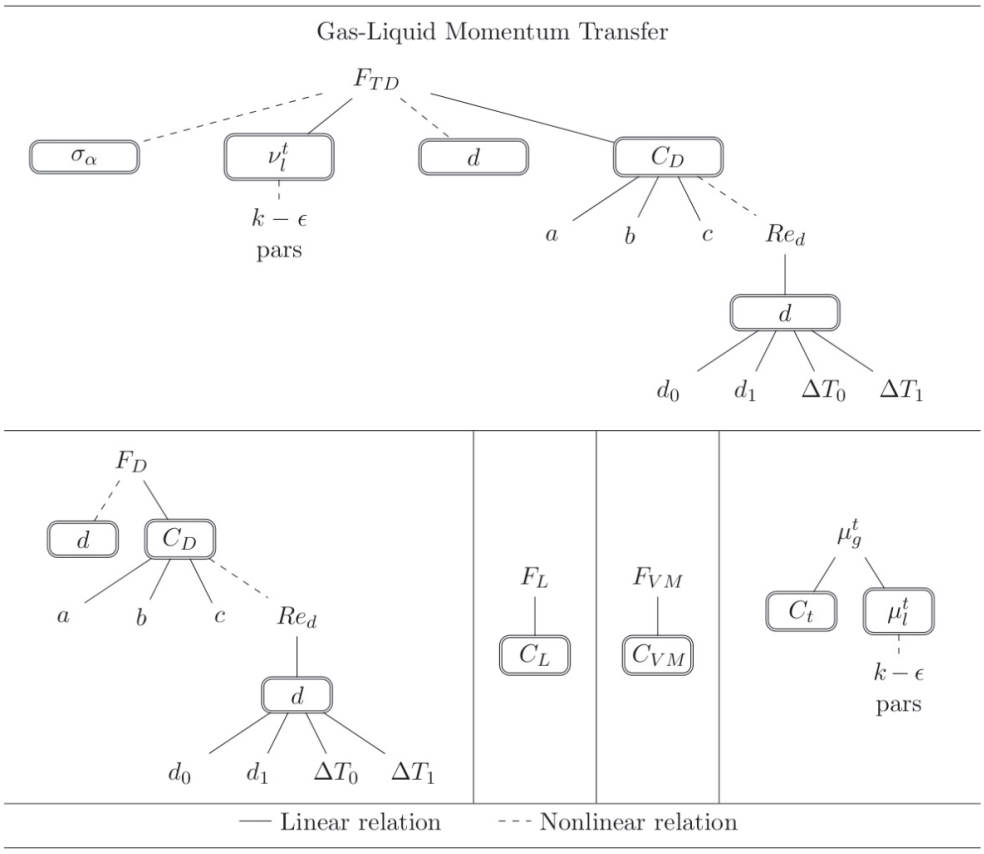

Figure 4. Momentum transfer models and parameters in STAR-CD

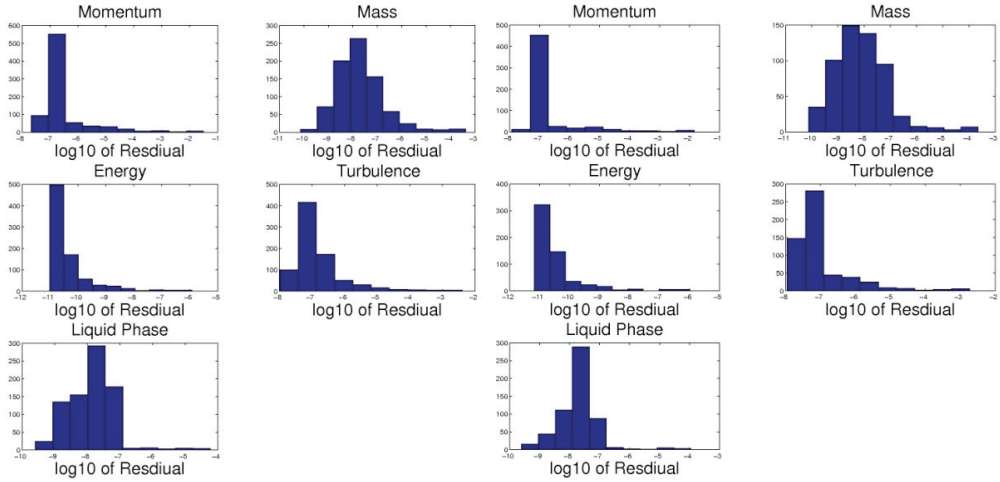

Figure 5. Histogram of residuals for each equation for heat partitioning model (left) and Chen s correlation (right)

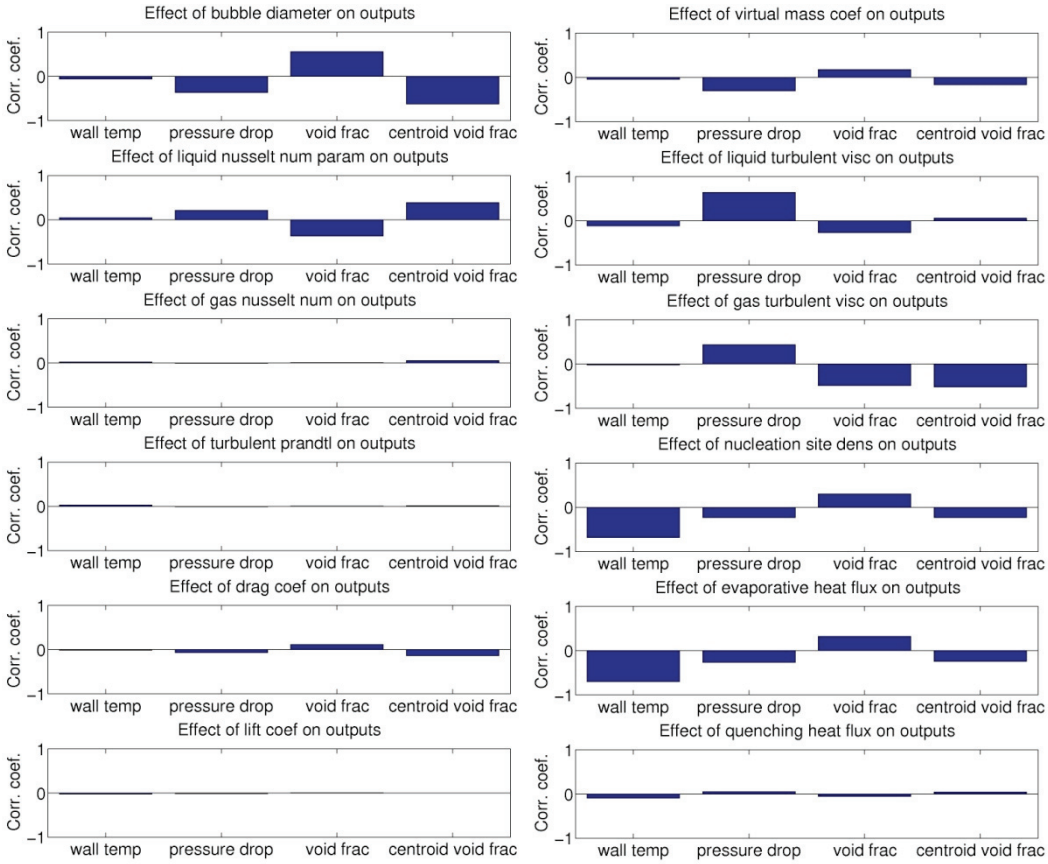

Figure 6. Correlation coefficients between parameters and outputs for heat partitioning model

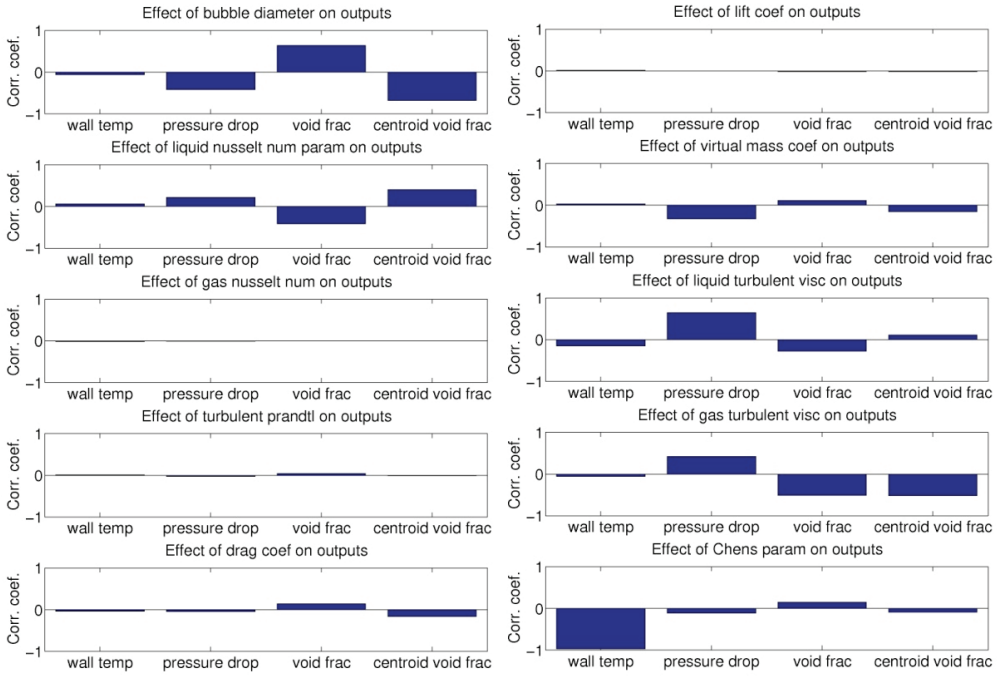

Figure 7. Correlation coefficients between parameters and outputs for Chen s correlation

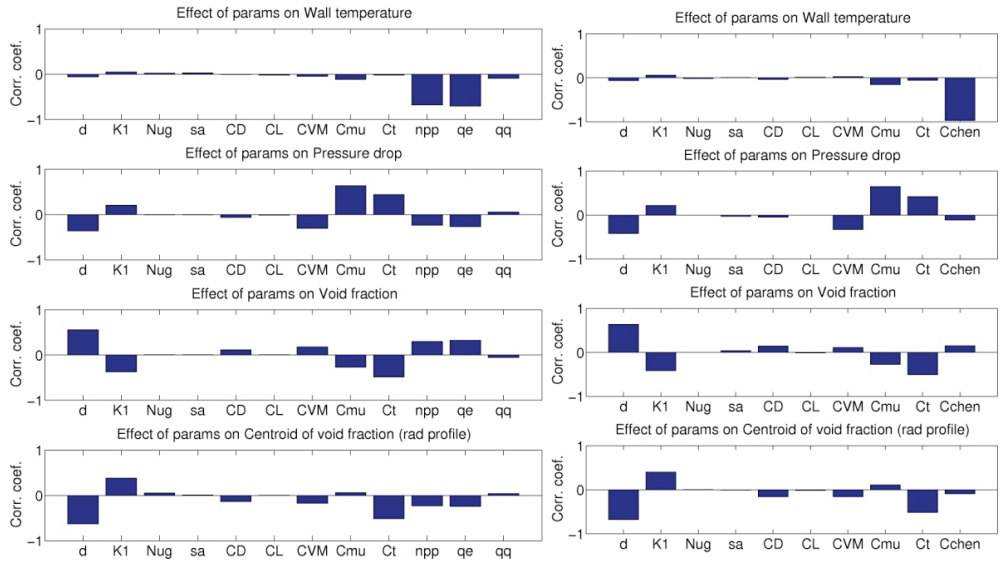

Figure 8. Correlation coefficients between outputs and parameters for heat partitioning model (left) and Chen s correlation (right)

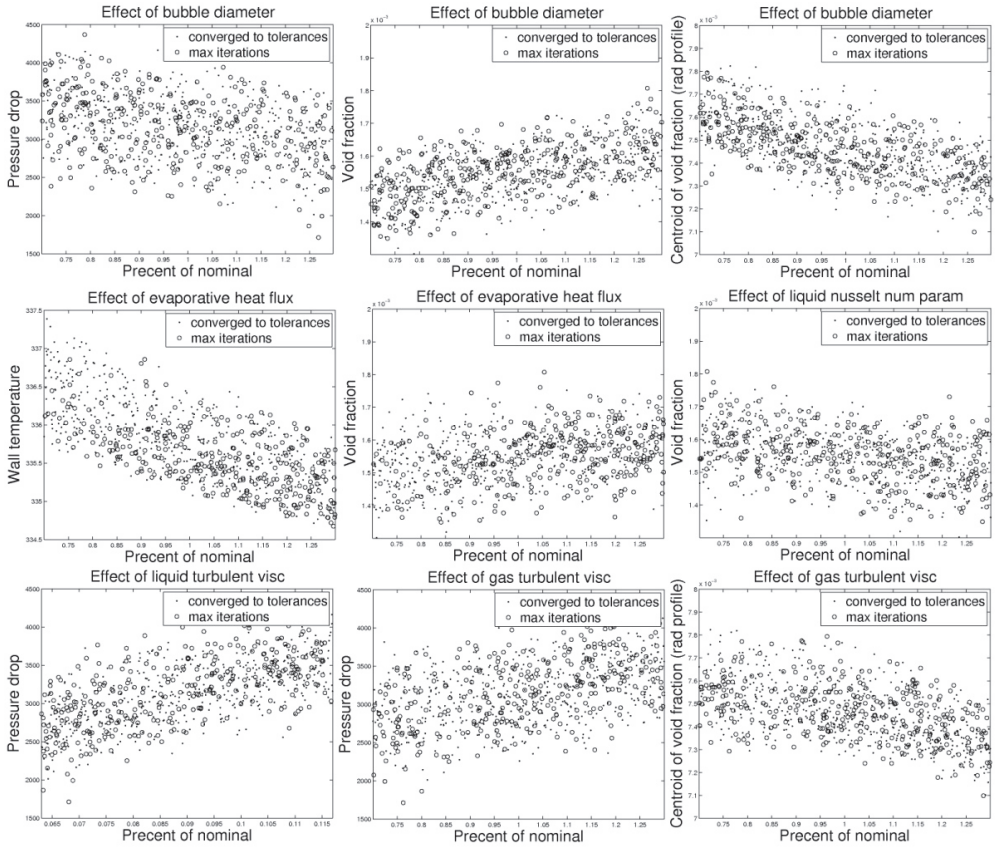

Figure 9. Selected scatter plots of parameter values versus outputs for heat partitioning model

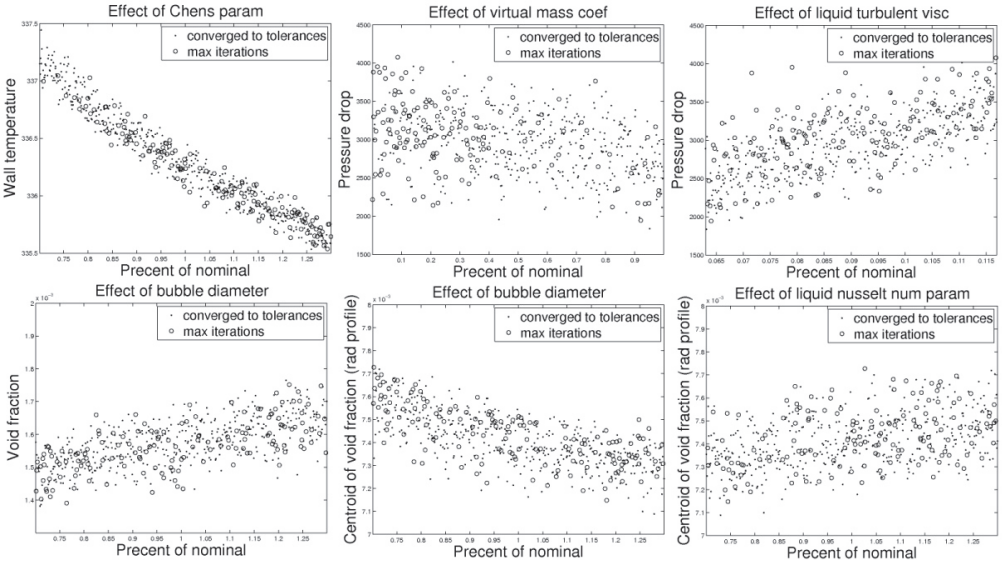

Figure 10. Selected scatter plots of parameter values versus outputs for Chen s correlation

7. SUMMARY AND CONCLUSIONS

This paper presents the results of a mesh convergence and a sensitivity study of boiling, multiphase, and turbulence models in thermalhydraulics simulations. Most of the models considered, with the exception of a new boiling correlation, are the defaults implemented in the commercial software package chosen for this study, STAR-CD.

The target problem is a simulation of the DEBORA-10 experiment of R-12 flowing through a vertical pipe with a heated test section. Outputs of interest consist of axial pressure drop, average wall temperature in the heated section, average void fraction at the end of the heated section, and the centroid of the radial distribution of the void fraction at the end of the heated test section. Sensitivity results for this problem demonstrate that bubble diameter is the most important overall parameter affecting the chosen outputs. Parameters governing the wall boiling model also show significant correlation with the outputs, with evaporative heat flux dominating the other terms in the heat-partitioning model. Turbulence terms are relatively important as well, but phase-to-phase momentum transfer terms do not show significant effects on the outputs in this problem; however, regarding the lift coefficient, no firm conclusion is possible as the baseline value is small in magnitude relative to the plausible range. Finally, variations in the boiling model based on Chen's correlation have a similar effect on the wall temperature output and a reduced effect on other outputs when compared to variations in the heat-partitioning model.

These conclusions are based on studies for one target problem. The extent to which the results generalize to other geometries and flow conditions requires further study. Nevertheless, we expect that conclusions concerning some of the fundamental underlying processes, specifically the importance of bubble diameter [20] and boiling models, to remain valid for other simulations involving sub-cooled boiling. Directions for future work include similar investigations with more sophisticated models, including the wall treatment and associated models, accounting for experimental error in parameter calibrations, more accurate estimates of parameter variability, and additional mesh convergence analyses of boiling and multiphase models.

REFERENCES

[1] N. Kurul and M.Z. Podowski, "On the modelling of multidimensional effects in boiling channels," *ANS Proceedings, National Heat Transfer Conference, 1991*

[2] R.M. Podowski and D.A. Drew and R.T. Lahey Jr. and M.Z. Podowski,, "A Mechanistic Model of the Ebullition Cycle in Forced Convection Subcooled Boiling," *Proceedings of the 8th International Topical Meeting on Nuclear Reactor Thermal-Hydraulics*. Vol. 3, 1997.

[3] M.Z. Podowski, "Recent Development in the Modeling of Boiling Heat Transfer Mechanisms," *Proceedings of the 13th International Topical Meeting on Nuclear Reactor Thermal-Hydraulics*, 2009.

[4] G.H. Yeoh and J.Y. Tu "A Bubble Mechanistic Model for Subcooled Boiling Flow Predictions," *Numerical Heat Transfer*, Vol 45, 2004, pp 475—493.

[5] J.Y. Tu and G.H. Yeoh, "On numerical modelling of low-pressure subcooled boiling flows," *International Journal of Heat and Mass Transfer*, Vol 45, 2002, pp 1197—1209.

[6] Bostjan Koncar and Eckhard Krepper, "CFD Simulation of Convective Flow Boiling of Refrigerant in a Vertical Annulus," *Nuclear Engineering and Design* 238, 2008, pp 693—706.

[7] Krepper, E., Koncar, B., Egorov, Y., 2007. "CFD modelling of subcooled boiling—concept, validation and application to fuel assembly design," *Nuclear Engineering and Design* 237, 716–731.

[8] Koncar, B., Matkovic, M., 2012. "Simulation of turbulent boiling flow in a vertical rectangular channel with one heated wall," *Nuclear Engineering and Design* 245, 131–139.

[9] Estrada-Perez, C.E., Hassan, Y., 2010. "PTV experiments of subcooled boiling flow through a vertical rectangular channel," *Int. J. Multiphase Flow* 38, 691–706.

[10] E. Krepper and R. Rzehak. "CFD for subcooled flow boiling: Simulation of DEBORA experiments," *Nuclear Engineering and Design* 241:3851–3866, 2011.

[11] J. Garnier, E. Manon, and G. Cubizolles, "Local Measurements on Flow Boiling of Refrigerant 12 in a Vertical Tube," *Multiphase Science and Technology*, Vol. 13, 2001, pp.1-111.

[12] S. Lo, A. Splawski, and B.J. Yun. "The importance of correct modelling of bubble size and condensation prediction of sub-cooled boiling flows," *Fourteenth International Topical Meeting on Nuclear Reactor Thermal Hydraulics*, 2011.

[13] STAR-CD Version 4.14 Methodology Manual, Chapter 13, CD-adapco, 2010.

[14] V. Ustinenko, M. Samigulin, A. Ioilev, S. Lo, A. Tentner, A. Lychagin, A. Razin, V. Girin, Ye. Vanyukov, "Validation of CFD-BWR, a new two-phase computational fluid dynamics model for boiling water analysis," *Nuclear Engineering and Design* 238, 2008, pp 660-670.

[15] Wang, D.M. 1994. 'Modelling of bubbly flow in a sudden pipe expansion', *Technical Report II-34*, BRITE/EuRam Project BE-4098.

[16] A.D. Burns, T. Frank, I. Hamill, and J.-M. Shi. "The Favre averaged drag model for turbulence dispersion in Eulerian multi-phase flows," *5th international conference on multiphase flow, ICMF2004*, Yokohama, Japan, 2004.

[17] Ranz, W.E., and Marshall, W.R. "Evaporation from drops — Parts I and II", *Chem. Eng. Prog*., 48(3), 1952, p. 141.

[18] M. Ishii and T. Hibiki, *Thermo-Fluid Dynamics of Two-Phase Flow*, Springer 2006.

[19] V.I. Tolubinsky and D.M. Kostanczuk, "Vapour Bubbles Growth Rate and Heat Transfer Intensity at Subcooled Water Boiling," Proc. 4th International Heat Transfer Conference, Vol. 5, 1970.

[20] S. Lo, A. Splawski, and B.J. Yun. "The importance of correct modelling of bubble size and condensation prediction of sub-cooled boiling flows," *Fourteenth International Topical Meeting on Nuclear Reactor Thermal Hydraulics*, 2011.